AIP | Applied Physics Letters

Wideband optical modulation via the magneto–optic interaction in a bismuth-lutetium-iron garnet film

A. Prabhakar and D. D. Stancil

Citation: Appl. Phys. Lett. **71**, 151 (1997); doi: 10.1063/1.119487
View online: http://dx.doi.org/10.1063/1.119487
View Table of Contents: http://apl.aip.org/resource/1/APPLAB/v71/i2
Published by the American Institute of Physics.

Wideband optical modulation via the magneto–optic interaction in a bismuth-lutetium-iron garnet film

A. Prabhakar
Department of Physics, Carnegie Mellon University, Pittsburgh, Pennsylvania 15213

D. D. Stancil
Electrical and Computer Engineering, Carnegie Mellon University, Pittsburgh, Pennsylvania 15213

(Received 3 March 1997; accepted for publication 6 May 1997)

Optical modulation with a bandwidth of about 3 GHz centered at 5.75 GHz was observed in a thin film of $[BiLu]_3Fe_5O_{12}$ using the magneto-optical interaction. A microstrip transducer was placed in contact with the film and TM polarized optical guided modes were excited beneath and parallel to the transducer. The TM→TE mode conversion was measured as a function of the angle between an in-plane field, of up to 100 Oe, and the optical beam. The bandwidth of the modulation was limited by the microwave components used in the external circuit. The experiments qualitatively agree with a simple model that describes a modulation of the optical beam by a nonresonant precession of the magnetization about an equilibrium.
[S0003-6951(97)00828-0]

Many optical components have been demonstrated in magnetic garnet thin films, leading to speculation that complete optical integrated circuits could be realized in these materials.[1–3] The first magnetic garnet waveguide modulator used a meandering current element to control the conversion between transverse electric (TE) and transverse magnetic (TM) optical modes.[1] The period of the meandering element was used to compensate for the phase mismatch between the TE and TM modes. The bandwidth of this device was limited by the retardation effects along the meandering elements. Optical modulation has been achieved using the interaction between magnetostatic waves and guided optical modes.[4,5] Bandwidths upto 1 GHz have been achieved with this technique.[6] Finally, high frequency modulation of light using oscillating periodic domain lattices has also been reported[7] where the bandwidth is determined by the resonant frequencies of the domain lattice.

In this letter, we modulate an optical guided mode over a bandwidth of 3 GHz using the driven, nonresonant precession of the magnetization in a garnet film. In some films, a large static mode conversion between the TE and TM modes is observed owing to the compensating effects of shape and stress-induced birefringence. This effect has been used to realize optical isolators.[8,9] By placing such a film in physical contact with a current carrying microstrip transducer, we cause a precession in the magnetization that in turn results in a modulation of the mode conversion. The interaction has a large bandwidth because of the nonresonant nature of the precession.

We use the experimental geometry shown in Fig. 1 to develop a simple model for the nonresonant modulation of a guided optical mode using an external microwave signal. A ferrimagnetic garnet film exhibiting some static TM↔TE optical mode conversion is placed in physical contact with a microstrip transducer. A TM polarized optical beam is edge coupled into a region of the film close to the transducer. The intensity of the modulated TE polarized light is measured as the output.

For purposes of simplicity, let the microstrip have a circular cross-section. With the reference direction for the current I taken to be along $-\hat{z}$, the magnetic field is given by

$$\boldsymbol{h}(x,y)=\frac{Ie^{j\omega t}}{2\pi\sqrt{x^2+y^2}}(\hat{x}\cos\phi+\hat{y}\sin\phi). \tag{1}$$

If the optical beam is far from the transducer (about 100 μm), $\phi\rightarrow 0$ and $\boldsymbol{h}$ is almost perpendicular to the plane of the film. Assuming $x_0^2 \ll y_0^2$, and neglecting any variations in $\boldsymbol{h}$ over the optical beam width, we estimate the value of the magnetic field at the center of the optical beam as

$$\boldsymbol{h}_0\approx\frac{Ie^{j\omega t}}{2\pi y_0}\hat{x}. \tag{2}$$

Let us now assume that the equilibrium magnetization of the film has no component perpendicular to the film and lies entirely in the $y-z$ plane. Figure 2 is a schematic showing the precession of the saturation magnetization $\boldsymbol{M}_s$ in the film about an equilibrium direction. We write the net magnetization as a sum of static and dynamic components, $\boldsymbol{M}=\boldsymbol{M}_s+\boldsymbol{m}e^{j\omega t}$ and use the Landau–Lifshitz equation to obtain

$$j\omega\boldsymbol{m}=\gamma\mu_0\boldsymbol{M}_s\times\boldsymbol{h}+O(\boldsymbol{m}\times\boldsymbol{h}). \tag{3}$$

Here, $\gamma=-2\pi$(28 GHz/T) is the gyrotropic ratio and μ_0 is the permeability of free space. In the presence of a weak

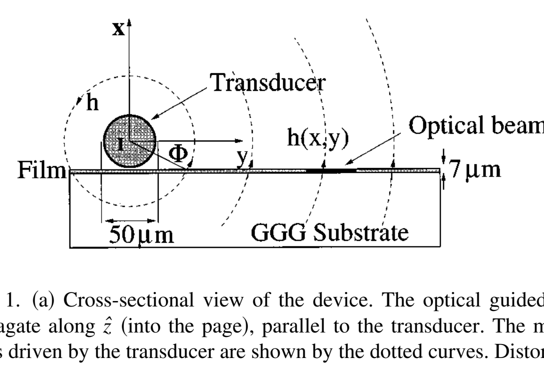

FIG. 1. (a) Cross-sectional view of the device. The optical guided modes propagate along $\hat{z}$ (into the page), parallel to the transducer. The magnetic fields driven by the transducer are shown by the dotted curves. Distortions in the field caused by the film are neglected.

 0003-6951/97/71(2)/151/3/$10.00

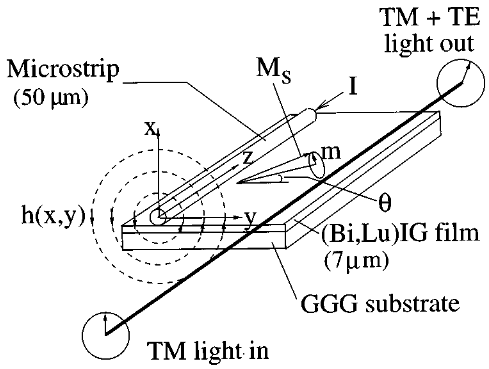

FIG. 2. Schematic of the device geometry. The in-plane magnetization precesses about an equilibrium direction defined by the angle with respect to $\hat{y}$.

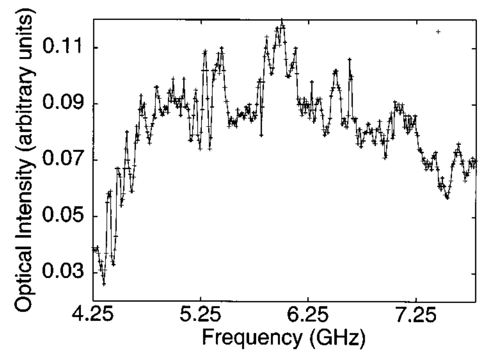

FIG. 3. Wideband modulation of the magneto–optic (MO) interaction. The frequency range of the interaction was limited by a 4–8 GHz microwave circulator.

external field $|\boldsymbol{H}| \ll |\boldsymbol{M}_s|$, the correction to (3) is $O(\boldsymbol{m}\times\boldsymbol{H})$ and can also be neglected. With $\boldsymbol{M}_s = M_s[\hat{y}\cos\theta + \hat{z}\sin\theta]$ and substituting (2) into (3), we get

$$\boldsymbol{m} = \frac{-j\gamma\mu_0}{\omega}\frac{IM_s}{2\pi y_0}[\hat{y}\sin\theta - \hat{z}\cos\theta]. \tag{4}$$

The relative permittivity tensor element ϵ_{yx} determines the TM→TE coupling for our device geometry. The dominant contribution to ϵ_{yx} is due to Faraday rotation and has the familiar form[10]

$$\epsilon_{yx} = -jfm_z + O(m_y m_z, m_z^2), \tag{5}$$

where f is an experimentally measured phenomenological parameter determined by the Faraday rotation[3,11] $\Phi_F = fM_s\pi/\lambda_0 n$, λ_0 is the optical wavelength, and n is the refractive index of the medium. The intensity, I_{MO}, of the TE mode at the output of the device is proportional to $|\epsilon_{yx}|^2$. Hence,

$$I_{MO} \propto |m_z|^2 \Rightarrow I_{MO} \propto \cos^2\theta. \tag{6}$$

This dependence on θ is intuitively correct. The intensity of the TE polarized light is a measure of the small signal magnetization and we expect I_{MO} to be a maximum when $\boldsymbol{M}_s$ is oriented in a direction perpendicular to the direction of propagation of the optical modes.

The inclusion of smaller quadratic terms in ϵ_{yx}, arising from the Cotton–Mouton effect,[12] does not discernibly affect the monotonic dependence of I_{MO} on θ. In our simple model, the bandwidth of the device is limited by the $1/\omega$ dependence in (4). In any device that compensates for this frequency dependence, the observed bandwidth will be determined largely by the characteristics of the external microwave components. In the above analysis, we have assumed perfect phase matching between the TM and TE optical modes. A small static TM↔TE conversion is an indication of a large phase mismatch between the optical modes and would limit the efficiency of the device. A more complete model will have to account for the change in the magnitude of the static conversion as the magnetization in the film rotates.

We now use the geometry shown in Fig. 1 for our experiment and compare the results with our theoretical predictions. A $[\mathrm{BiLu}]_3\mathrm{Fe}_5\mathrm{O}_{12}$ film exhibiting a modest 2% static TM→TE conversion is placed in contact with the microstrip transducer. The microwave output of an oscillator is modulated with an audio signal and fed into the transducer. TM polarized light ($\lambda = 1.3$ μm) is edge coupled into the film and we measure the intensity of TE polarized light at the output. The optical modulation is observed by sending the signal from the detector to a lock-in amplifier with the audio signal as a reference. Figure 3 shows the ~3 GHz bandwidth that was obtained by this method. The bandwidth was limited by a 4–8 GHz circulator that was inserted before the transducer.

We were unsuccessful in our attempts to observe magnetic domain walls in the film using an optical microscope with crossed polarizers, suggesting that the magnetization was in the plane of the film. The microscope image did not change significantly when we applied a magnetic field (~100 Oe) perpendicular to the film plane. Similarly, in our experiments on the modulation, the output was unaffected by perpendicular fields upto 105 Oe.

When we apply an external microwave field, the magnetization begins to precess about its equilibrium direction. The dynamic magnetization causes TM→TE optical mode conversion which is measured by the lock-in amplifier. The orientation of the equilibrium direction determines the magnitude of this conversion and we control the orientation by applying a static external magnetic field. The field is generated by two perpendicularly oriented electromagnetic coils with independent power supplies. The device is mounted so that the magnetic field lies in the plane of the film and its direction is controlled by changing the current in each of the two coils. The experiment is conducted by incrementing H_z from 0 to 80 Oe in steps of 2.4 Oe and H_y from 0 to 105 Oe in steps of 5.3 Oe. The values chosen for the magnetic fields were determined by the capabilities of the controlling instrumentation and the power supplies of the two coils. Figure 4 shows a three-dimensional (3D) plot of the output as we change H_z and H_y with a microwave signal at 6 GHz. At weak values of the static field there are rapid variations due, perhaps, to the formation of domains. $H_y \to 105$ Oe, $H_z \to 0$ is a region of maximum interaction and $H_y \to 0$, $H_z \to 80$ Oe is a region of minimum interaction, an observation that supports our model.

In Fig. 5, we ignore the influence of $|\boldsymbol{H}|$, and express the data from Fig. 4 as a function of the equilibrium direction,

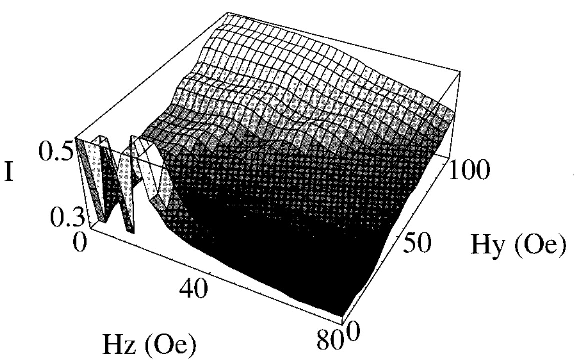

FIG. 4. Change in the wideband interaction intensity, I_{MO} (in arbitrary units), as the external magnetic fields H_z and H_y are varied. Grey scales are used to denote the relative interaction intensity with white representing the maximum and black the minimum. The microwave frequency was 6 GHz.

calculated as $\theta = \tan^{-1}(H_z/H_y)$. We also ignore the rapid variations in I_{MO} close to the origin in Fig. 4, where $|\boldsymbol{H}| \rightarrow 0$. The data in Fig. 5 have been normalized with respect to the maximum interaction at $\theta = 0$. The overall envelope of the data is qualitatively consistent with the $\cos^2\theta$ behavior predicted by (6) and shown by the dotted curve.

Figure 5 reveals some unexpected features in the wideband interaction. Local minima occur at particular values of θ. This nonmonotonic output optical intensity cannot be explained by our present model. The minima in I_{MO} are seen as ripples radiating outward from the origin in Fig. 4, and occur at $\theta =$ 0.5, 0.7, and 0.85 rad. Furthermore, the data in Fig. 5 appear to fall into three distinct regions, each region having a finite width. Region 1 corresponds to the strongest external magnetic field, which at $\theta = 0$ matches the condition $|\boldsymbol{H}| = H_y = 105$ Oe. For $\theta < 0.75$ rad, the strong magnetic field tends to destroy the nonmonotonic behavior of I_{MO}. The finite width of a region is possibly due to the discrete values for H_y and H_z that causes a spread in the value of $|\boldsymbol{H}|$, consequently causing a spread in I_{MO}. Other probable effects contributing to a nonmonotonic behavior and a grouping of data into regions are magnetic anisotropy in the film plane and variations in the film birefringence owing to the equilibrium direction of $\boldsymbol{M}_s$.

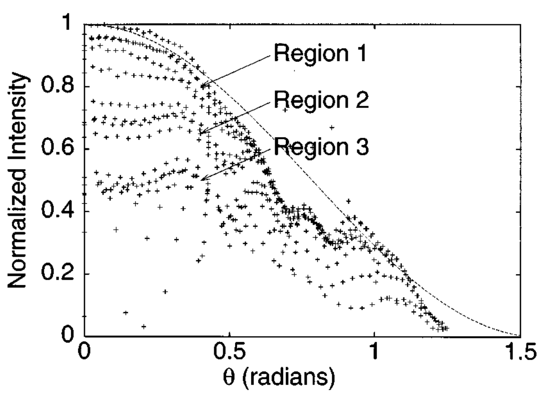

FIG. 5. Change in the wideband interaction intensity as the equilibrium magnetization direction is changed with respect to the optical beam. The distinct regions are attributed to the different levels of magnetic saturation as we change $|\boldsymbol{H}|$.

In summary, a wide bandwidth modulator is an important component of an integrated optical technology based on magnetic garnet thin films. We have demonstrated a new magneto-optical modulator with a bandwidth of about 3 GHz centered at 5.75 GHz. This bandwidth was limited by the microwave components in our experiments. Based on a simple model of nonresonant precession, the amplitude of our signal is expected to be inversely proportional to the operating frequency. However, it should be possible to compensate for this decrease over a multi-gigahertz range using a properly designed microwave drive circuit. The presence of a weak static external magnetic field helps stabilize the device while the orientation of the field gives some control over the gain of the modulation.

[1] P. K. Tien, R. J. Martin, R. Wolfe, R. C. Le Craw, and S. L. Blank, Appl. Phys. Lett. **21**, 8,394 (1972).

[2] B. Neite and H. Dotsch, Proc. SPIE **1018**, 115 (1988).

[3] D. D. Stancil, IEEE J. Quantum Electron. **27**, 61 (1991).

[4] A. D. Fischer, J. N. Lee, E. S. Gaynor, and A. B. Tveten, Appl. Phys. Lett. **41**, 779 (1982).

[5] C. S. Tsai, D. Young, W. Chen, L. Adkins, C. C. Lee, and H. Glass, Appl. Phys. Lett. **47**, 651 (1985).

[6] D. Young and C. S. Tsai, Appl. Phys. Lett. **53**, 1696 (1988).

[7] K. Blanke, B. Luhrmann, U. Wallenhorst, H. Dotsch, and W. Tolksdorf, Phys. Status Solidi A **124**, 359 (1991).

[8] H. Dammann, E. Pross, G. Rabe, W. Tolksdorf, and M. Zinke, Appl. Phys. Lett. **49**, 1755 (1986).

[9] R. Wolfe, V. J. Fratello, and M. McGlashan-Powell, J. Appl. Phys. **63**, 3099 (1988).

[10] A. M. Prokhorov, G. A. Smolenskii, and A. N. Ageev, Sov. Phys. Usp. **27**, 339 (1984).

[11] H. Tamada, M. Kaneko, and T. Okamoto, J. Appl. Phys. **64**, 554 (1988).

[12] R. V. Pisarev, I. G. Sinaii, and A. G. Smolenski, Sov. Phys. JETP **9**, 112 (1969).